Semnan University

Journal of Sustainable Energy & Chemical Engineering

Journal homepage: https://SECE.semnan.ac.ir/

Research Article

A kinetic model for carbothermal reduction of iron oxides in a carbon containing composite pellet

Ehsan Baghshani [a]*

[a] *Sadaf Petrochemical Company, Persian Gulf Petrochemical Industries Holding, Asaluyeh, 1993873050, Iran*

ARTICLE INFO

Article history:

Received: 202*-**-**

Revised: 202*-**-**

Accepted: 202*-**-**

Keywords:

Iron oxide reduction;
carbothermal;
mathematical modeling;
reduction reaction kinetics.

ABSTRACT

Today, among the various methods of iron oxide reduction, direct reduction methods, including the carbothermal reduction method, have been favored by industries around the world due to their advantages such as low energy consumption and low pollution compared to other reduction methods. In the present study, a mathematical model is developed to simulate the kinetics of the reduction reaction of iron oxide dust and carbon composite pellet in a rotary hearth furnace and consequently, investigate the behavior of the process in variations of the pellet carbon content. The model results were in a good consistent with experimental results. Calculating results showed that with increasing the C/O ratio that was varied from 0.5 to 2.53, the temperature profile inside the pellet forms in a shorter time due to the increase of effective thermal conductivity of the composite and consequently reaction zones start sooner. As it was seen , the percentage of deoxygenation for a change in carbon content of 0.5 to 2.53 increased from 0.27 to 0.71, respectively. Since there is a carbon lost through exiting the gases from the pellet; stoichiometric ratio of C/O cannot complete the total metallization of the iron oxides. Therefore, the C/O ratio higher than unity is required for completion of reduction.

*** Corresponding author.**
E-mail address: baghshaniehsan@gmail.com

Cite this article as:

Baghshani E. (2025). A kinetic model for carbothermal reduction of iron oxides in a carbon containing composite pellet. *Journal of Sustainable Energy & Chemical Engineering*, Vol. (No.), pp. 1-27.

https://doi.org/10.22075/SECE.2023.24860.1004

1. Introduction

Steelmaking industry is of the great importance due to its excellent accessibility and widespread usage in modern communities [1]. On the other hand, steelmaking companies face low efficiency, and high energy costs and environmental challenges of carbon emissions [2, 3]. Therefore, optimizations and characterization of process and its behaviors have become important in the research and development point of view. Figuring out how to promote the product quality and optimizations in the iron oxide reduction can dramatically improve the performance of steel making industry. Currently, 90 % of the steel produced worldwide is produced by the blast furnace process. On the way from mining to production in the furnace, 3.8 billion tons of iron oxide dust are produced by mining erosion and abrasion, which blast furnace process cannot process this dust to steel [4]. Since producing the metal iron from its oxides is an energy consuming process, direct reduction process that reduces iron oxides directly in solid phase has been developed. Carbothermic reduction on the other hand is an environment friendly technique that has been developed due to its low carbon emission and low energy consuming characteristic in direct iron oxide reduction process [5, 6]. In carbothermic reduction the powders of Iron oxide and carbon as reducing agents are in contact with a large contact surface, and at temperatures of 1100 to 1300 degrees Celsius, the reduction occurs rapidly [7]. Hence, it's a complicated process affected by many parameters and occurring reactions controlled by heat and mass transfer. Optimizing such multiparameter process through experimentation is time consuming and a costly effort. Therefore, the development of a mathematical modeling could describe carbothermal reduction of iron oxide have been always an essential matter to the researchers through last decades.

Sun and Lu [8] developed a mathematical model to assess the kinetic behavior of carbothermal reduction of iron oxides dusts in an ore-coal composite pellet. Their results confirmed that the overall endothermic reactions of reduction are limited with heat transfer especially heat conduction from the wall through the center of the pellet. Maroufi et al. [9] were investigated the carbothermal reduction of iron and silicon oxides from the ironstone ore. They carried out the reduction in a temperature up to 1400 ℃ to reach the sponge iron and ferrosilicon. Pistorius [10] studied the carbothermic reduction of iron oxides using the temperature limiting as a controller of reduction rates. Leuchtenmüller et al. [11] modeled the carbothermic reduction of zinc oxide from the industrial wastes in order to optimize the reduction conditions and they reached the recovery of metallic zinc from it oxides over the 99%. Zinoveev et al. [12] studied the carbothermic reduction of red mud as an iron oxide rich waste matter from the aluminum production process. They obtained the ability to extract the magnetic reduced iron from the red

mud and cost-effectively purified the metallic iron through the carbothermic reduction and magnetic field aided purification process.

The behavior of carbothermic reduction of iron oxides is complicated and mechanisms dominating the kinetics, mass and energy transfer phenomena are complex leading to understanding the impacts of operating conditions on the efficiencies too difficult. In order to process evaluations, the experimental study takes time and is costly. However, presentation of a mathematical model describing the behavior of the process is a strong and reliable technique to predict the process characteristics and it is a cost-effective method to optimize operating conditions. In this study the effect of carbon content in composite iron oxide pellet as the most important parameter affecting the process behavior was investigated.

2. Mathematical model

2.1. Pellet model

The iron oxides and carbon composite pellet was considered as a perfect porous sphere and assumed its radius did not change during the reaction. The pellet is placed in the furnace under radiation and the heat is conducted from the pellet wall into its center. Reactions were started as the pellet layers reached into the considerable temperatures. Solid-state reactions of Boudouard and carbothermal reductions are carried out by the diffusion of gaseous intermediates through the porous media of the pellet. During the reaction proceed, the porosity of pellet was increasing due to the carbon gasification, and oxygen removal from iron oxides in the solid phase. Also, in the conservation equations, the variations are considered only in the radial dimension and variations in other dimensions were neglected.

2.2. Reactions

The reactions considered to be dominate the reduction of iron oxide process are listed in relations 1to 11 that proposed by Kuwauchi [13].

$$3Fe_2O_3 + CO = 2Fe_3O_4 + CO_2 \quad (1)$$
$$3Fe_2O_3 + H_2 = 2Fe_3O_4 + H_2O \quad (2)$$
$$1.202\ Fe_3O_4 + CO = 3.807\ FeO + CO_2 \quad (3)$$
$$1.202\ Fe_3O_4 + H_2 = 3.807\ FeO + H_2O \quad (4)$$
$$0.25Fe_3O_4 + CO = 0.75Fe + CO_2 \quad (5)$$
$$0.25\ Fe_3O_4 + H_2 = 0.75\ FeO + H_2O \quad (6)$$
$$Fe_{0.974}O + CO = 0.974\ Fe + CO_2 \quad (7)$$
$$Fe_{0.974}O + H_2 = 0.974\ Fe + H_2O \quad (8)$$
$$C + CO_2 = 2CO \quad (9)$$
$$C + H_2O = CO + H_2 \quad (10)$$
$$CO + H_2O = CO_2 + H_2 \quad (11)$$

The reaction rate equations used in this study not mentioned here for the sake of brevity. The detailed descriptions can be found in Kuwauchies work [13].

2.3. Mass & energy conservation equations

The concentration changes of the reactive species in the gas and solid phases are obtained using equations 12 and15 respectively. The gas diffuses and reacts due to the concentration difference. The gas diffusion is obtained from the Fick equation and the effective diffusion coefficient. The solid species changes occur only by the production and consumption reactions.

$$\frac{\partial C_k}{\partial t} = \frac{1}{r^2}\frac{\partial}{\partial r}\left(r^2 D_{eff}\frac{\partial C_k}{\partial r}\right) - rxn_k \tag{12}$$

The boundary conditions for solving equation 12 are obtained from equations 13 and 14.

$$D_{eff}\frac{\partial C_k}{\partial r}\Big|_{r=surface} = k_g\left(C_{k,f} - C_{k,l}\right) \tag{13}$$

$$\frac{\partial C_k}{\partial r}\Big|_{r=center} = 0 \tag{14}$$

Were C_k is concentration of gas compositions, D_{eff} is effective diffusion coefficient and k_g is the mass transfer coefficient.

$$\frac{\partial \rho_k}{\partial t} = -rxn_k \tag{15}$$

Were ρ_k is the concentration of solid components. The energy conservation in pellet follows the equation 16.

$$\rho C_p\frac{\partial T}{\partial t} = \frac{1}{r^2}\frac{\partial}{\partial r}\left(r^2\lambda_{eff}\frac{\partial T}{\partial r}\right) - rxn.\Delta H_{rxn} \tag{16}$$

Were λ_{eff} is the effective conductivity of porous media of pellet. The boundary conditions for equation 16 are represented in equations 17&18.

$$\lambda_{eff}\frac{\partial T}{\partial r}\Big|_{r=surface} = \varepsilon\sigma\left({T_{furnace}}^4 - {T_{surface}}^4\right) \tag{17}$$

$$\frac{\partial T}{\partial r}\Big|_{r=center} = 0 \tag{18}$$

σ is Stefan-Boltzmann constant. ε is emissivity of pellet surface.

2.4. Properties

The porosity of pellet was obtained by calculating the volume of each solid phase species through dividing the masses by their densities, then subtracting their summation from the unity as described in equation 19.

$$\varphi = 1 - \frac{\mathrm{W}}{\mathrm{V}} \sum_{j=1}^{n} \frac{C_j}{d_j} \tag{19}$$

Were φ is the porosity of pellet. W and V are pellet mass and volume respectively. d_j is the density of pellet components. The effective intra-pellet diffusion coefficient, depending on the gas components in the pores, temperature, pressure, and porosity is obtained using equations 20 to 22.

$$D_{kl} = D_{kl\,0} \cdot \left(\frac{T}{273}\right)^{m_{kj}} \left(\frac{1.01325\times10^5}{P_t}\right) \tag{20}$$

D_{kl} is the temperature & pressure dependent diffusion coefficient of gaseous component k in gaseous component l. The diffusion coefficient of component k in gaseous mixture (D_k) is calculated with equation 21.

$$D_k = \frac{P_t}{\sum_l \frac{P_l}{D_{kl}}} \tag{21}$$

The diffusion coefficient of component k in a porous media is corrected with equation 22.

$$D_{eff,k} = \frac{2\varphi}{3-\varphi} D_k \tag{22}$$

The effective thermal conductivity is obtained using the thermal conductivity of the gas mixture components and solid phase components with the correction of porosity using equations 23 to 26.

$$\lambda_{gas} = \frac{\sum_k \lambda_k P_k {MW_k}^{1/3}}{\sum_k P_k {MW_k}^{1/3}} \tag{23}$$

$$\lambda_{solid} = \prod_j {\lambda_j}^{V_j} \tag{24}$$

$$\lambda_{eff} \begin{cases} \lambda_{solid} \times \dfrac{1+2\alpha\varphi}{1-\alpha\varphi} & (\varphi \le 0.1) \\ \lambda_{gas} \times \dfrac{1+2\beta(1-\varphi)+(2\beta^3-0.1\beta)(1-\varphi)^2+0.05(1-\varphi)^3 e^{4.5\beta}}{1-\beta(1-\varphi)} & (0.1 < \varphi \le 0.9) \\ \lambda_{gas} \times \dfrac{1+2\beta(1-\varphi)}{1-\beta(1-\varphi)} & (0.9 < \varphi) \end{cases} \tag{25}$$

Which the parameters $\alpha\&\beta$ are calculated from equations 26.

$$\alpha = \frac{\lambda_{gas} - \lambda_{solid}}{\lambda_{gas} + 2\lambda_{solid}} \qquad \beta = \frac{\lambda_{solid} - \lambda_{gas}}{\lambda_{solid} + 2\lambda_{gas}} \tag{26}$$

The heat capacity, enthalpy of reactions, kinetic parameters of the composite pellet were calculated as described in the Kuwauchi's study [13].

3. Results

The mathematical model described in the previous section was solved with finite volume method using MATLAB software. The conditions of program run are reported in Kuwauchi's work. The calculated results were compared with experimental data. The figure 1 shows calculated values from this study and measured values of reduction percentage reported in Kuwauchi's work [13].

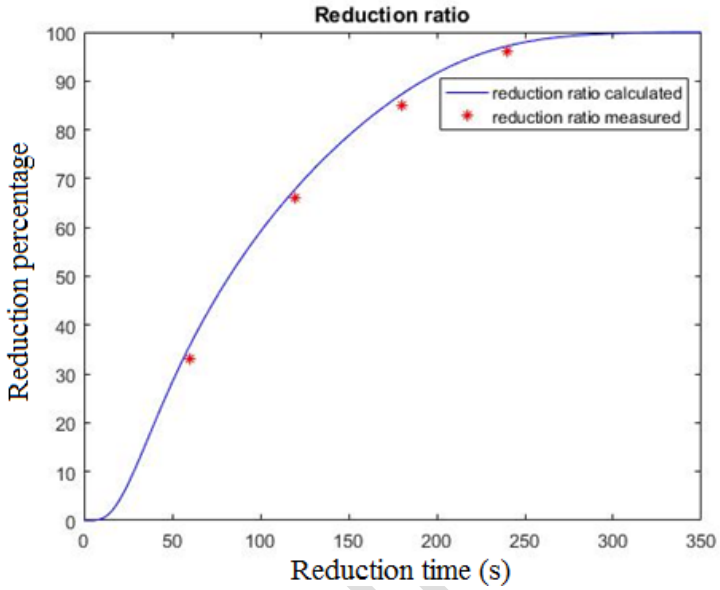

Fig. 1. Calculated and measured reduction percentage

The error for the values calculated from the simulation and the experimental was calculated by Equation 27 are reported in Table 1.

Only horizontal lines should be used within a table, to distinguish the column headings from the body of the table, and immediately above and below the table. Tables must be embedded into the text.

$$\text{Error} = \frac{|calculated - measured|}{measured} \tag{27}$$

Table 1. Error values for calculated and measured values

Time (s)	60	120	180	240
error	0.0843	0.0294	0.0265	0.0120

Equation 28 shows the overall reaction for the reduction of metal oxides (in this study, iron). The stoichiometry of reaction suggests the molar ratio of carbon to oxygen to be 0.5. But what occurs is that a part of the CO produced inside the pellet penetrates through it and exits the pellet wall without participating in the reaction.

$$M_xO_y + \frac{y}{2}C \rightarrow xM + \frac{y}{2}CO_2 \quad (28)$$

The impact of carbon ratio as a ratio of Carbon per overall oxygen existed in the mixture of iron oxides of pellet was investigated. Figure 2 shows the temperature profile inside the pellet for C/O values of 0.5, 1.54, 1.9 & 2.53. The scenario considered in the simulation was that the molar ratio of carbon to the total oxygen content of iron oxides was changed in the way that the total pellet mass and diameter were kept constant and equal to the conditions of model validation. These values were considered equal to 30 g and 3 cm, respectively.

As can be seen in figure 2 the temperature profile of the pellet improves with increase of C/O ratio due to increase the heat conductivity of composite pellet.

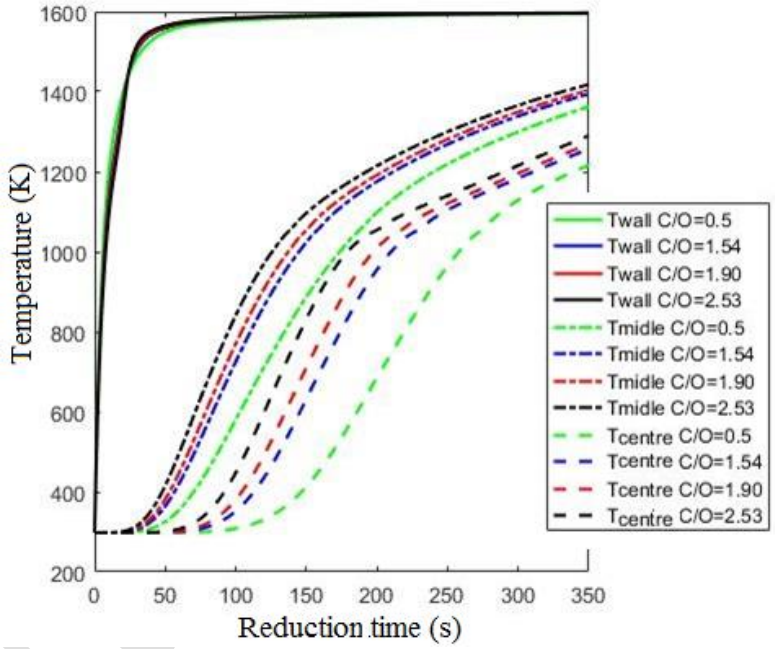

Fig. 2. Temperature profiles within the pellet for different carbon ratios

The variation of C/O ratio effects on the thermophysical properties including thermal conductivity, diffusivity and porosity during the reduction time. The thermal conductivity within the pellet depends on porosity, temperature, and the composition of the gas and solid phase components. It should also be noted that due to the change in solid and gas species and the non-uniform occurrence of reactions within the pellet, the porosity and thermal conductivity within the pellet were varied during the reaction time. Figures 3 & 4 show the variation of porosity and thermal conductivity inside the pellet respectively.

The simulation for C/O ratio of 0.5 showed the highest porosity among the others at the start of the reduction but it became the least porous composite at the end of reduction due to the least carbon gasification compared to other C/O ratios.

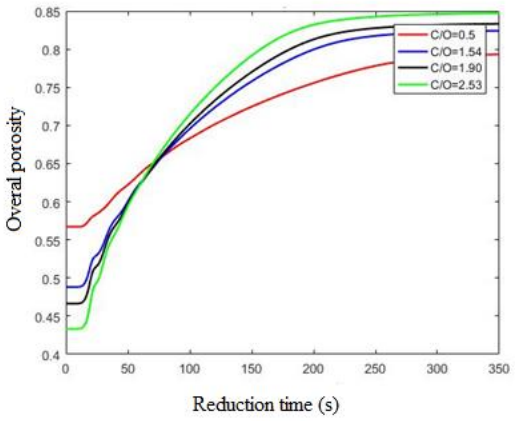

Fig. 3. The effect of C/O ratio on porosity.

Figure 4 also shows that the overall thermal conductivity of the pellet increases with increasing carbon content at the beginning of the reduction process. Also, the ascending part of the curve, which was attributed to pellet components and temperature, shifts upward by a constant value with increasing carbon content within the pellet, and passes a peak. It is also observed that the maximum value of the overall thermal conductivity of the pellet is shifted to the left and to earlier seconds of the process with increasing carbon ratio, which, as observed in the temperature distribution section, causes a faster development of the temperature distribution within the pellet and consequently reaching the desired temperature for initiating the reaction in the inner layers of the pellet. But as the reaction progresses, the porosity increases and consequently the thermal conductivity decreases, reaching the lowest value for the highest carbon ratio and the highest value for the lowest carbon ratio at the end of the reaction. However, it should be noted that at the final times, the temperature profile is formed and thermal conductivity has no effect on the reaction. Therefore, increasing thermal conductivity at times before the temperature distribution has developed has been beneficial.

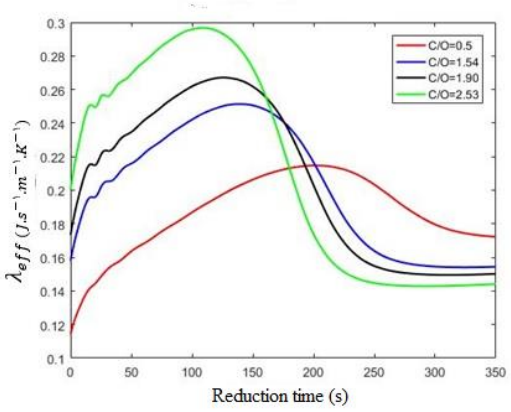

Fig. 4. The effect of C/O ratio on effective thermal conductivity.

Figures 5 and 6 show the effect of the carbon to oxygen ratio within the pellet on the reduction percentage and the thickness of the constant time oxygen removal curves representing the reaction zones, respectively. From figure 5 it can be realized that the reduction rate becomes steeper for higher carbon contents and the reaction proceeds faster. Also figure 6 shows that the effect of the carbon to oxygen ratio on the reduction of pellet layers is not the same, so that in the pellet wall, the carbon to oxygen ratio has less effect due to the rapid reaching of the desired reaction temperature, and the completion of the reduction in a small fraction of the reduction time. However, this effect becomes more intense in the middle and center of the pellet. This dependence on the carbon to oxygen ratio is determined by the width of the area enclosed between the curves between the lowest and highest carbon ratios for each layer of the pellet. It can be seen that at the time of 300 seconds, and the molar ratio of carbon to oxygen is equal to 0.5 at the center of the pellet; the fraction of oxygen removal reached 0.28, while for the highest carbon to oxygen ratio (equal to 2.53), this value has reached above 0.71.

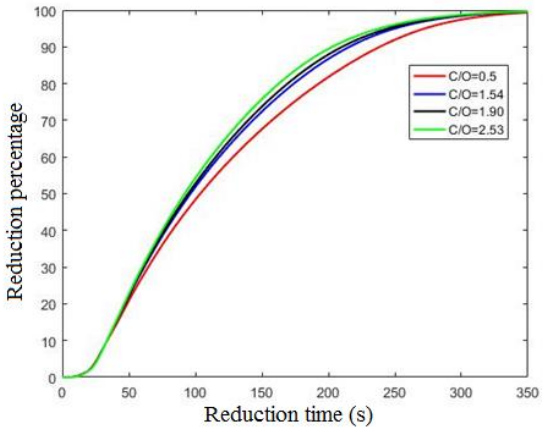

Fig. 5. The effect of C/O ratio on the reduction percentage within the pellet.

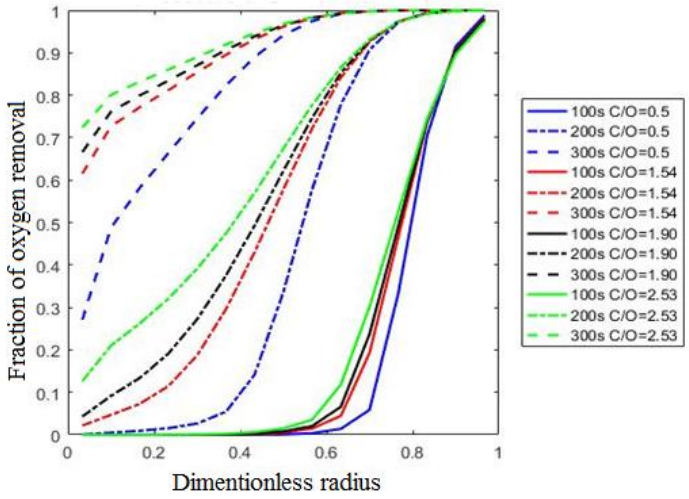

Fig. 6. Effect of C/O ratio on reaction zone thickness

4. Conclusion

A mathematical model for a carbothermal reduction of a composite pellet containing iron oxides dust and carbon powder was developed and solved to predict the process behavior. The calculating results showed a good consistent with the experimental results. The values of C/O ratio equal to 0.5, 1.54, 1.9 & 2.53 as an important parameter in the carbothermal reduction process were considered and the impact of C/O variation on process were evaluated. Increase the C/O ratio from 0.5 to 2.53 resulted in the temperature shift of the pellet center to from 1210°C to 1300°C at end of the simulation. During the reduction period, the heat conductivity increases with the start of the reaction and the metallization of the pellet, and after the porosity increases and the reduction reactions accelerate, the conductivity quickly falls. Increasing the C/O ratio causes the reactions to accelerate faster and more rapidly. Changing the C/O ratio from 0.5 to 2.53 shifted the beginning of reaction acceleration time from 220th seconds to 100th seconds. Increasing the C/O ratio increased the reaction area and dramatically increased the penetration rate of the reaction front, such that at the end of the simulation in the center of the pellet, the percentage of deoxygenation for a change in carbon content of 0.5 to 2.53 increased from 0.27 to 0.71, respectively.Increasing the carbon to oxygen ratio at the end of the reaction causes a decrease in the degree of iron purity and the formation of iron carbide, which is not beneficial to the reaction. The modeling result indicates that the carbon ratio of the pellet has a strong impact on the time of reduction and completion of the reaction. As was shown increasing the carbon improve the formation of temperature profile and reduced the reduction time. Also, the reaction zone distribution in different times of reduction was obtained aiding the process optimization and design. This study results shows the complicity of Iron oxide direct reduction

and strength and importance of mathematical modeling to represent the behavior of carbothermic reduction of Iron oxide.

References

[1] Zhou, D., Xu, K., Lv, Z., Yang, J., Li, M., He, F., Xu, G. (2022). Intelligent manufacturing technology in the steel industry of China: a review. *Sensors, 22, 8194.*

[2] Hayashi, M., Takeda, K., Kashimura, K., Watanabe, T., Nagata, K. (2013). Carbothermic reduction of hematite powders by microwave heating. *ISIJ international. 53, 1125-1130*

[3] d'Izard, M.B., Abanades, S. (2025). Carbothermal reduction of hematite involving biogenic carbon sourced from CO2. *Chemical Engineering Journal Advances*. *100925*.

[4] Raj, R., Kumari, A., Sahu, D. K., Prasad, R., & Ranganathan, S. (2019). Carbothermic reduction of iron oxide waste generated during the processing of ilmenite. *Transactions of the Indian Institute of Metals, 72(1), 11-16.*

[5] Zare Ghadi, A., Radfar, N., Valipour, M. S., & Sohn, H. Y. (2023). A review on the modeling of direct reduction of iron oxides in gas-based shaft furnaces. *steel research international, 94(6), 2200742.*

[6] Chatterjee, A. (2010). Sponge iron production by direct reduction of iron oxide. *PHI Learning Pvt. Ltd.*

[7] Wang, G., Wang, J., & Xue, Q. (2018). Kinetics of the volume shrinkage of a magnetite/carbon composite pellet during solid-state carbothermic reduction. *Metals, 8(12), 1050*.

[8] Sun, K., & Lu, W. K. (2009). Mathematical modeling of the kinetics of carbothermic reduction of iron oxides in ore-coal composite pellets. *Metallurgical and Materials Transactions B, 40(1), 91-103.*

[9] Maroufi, S., Ciezki, G., Jahanshahi, S., & Ostrovski, O. (2016). Carbothermal reduction of iron and silicon oxides in ironstone ore. *Mineral Processing and Extractive Metallurgy, 125(2), 86-94.*

[10] Pistorius, P. C. (2005). Kinetics of carbothermic reduction reactions under heat transfer control: modelling results. *Scandinavian journal of metallurgy, 34(2), 122-130.*

[11] Leuchtenmüller, M., Legerer, C., Brandner, U., & Antrekowitsch, J. (2021). Carbothermic reduction of zinc containing industrial wastes: a kinetic model. *Metallurgical and Materials Transactions B, 52(1), 548-557.*

[12] Zinoveev, D., Pasechnik, L., Grudinsky, P., Yurtaeva, A., & Dyubanov, V. (2022). Kinetics and mechanism of red mud carbothermic reduction and reduced iron grain growth: an influence of sodium sulfate. *Crystals, 13(1), 1.*

[13] Kuwauchi, Y., & Barati, M. (2013). A mathematical model for carbothermic reduction of dust-carbon composite agglomerates. *ISIJ international, 53(6), 1097-1105.*